Triple differential cross sections for electron-impact ionization of He^+

Xingfu Jia,[1] Qicun Shi,[2] Zhangjin Chen,[2] Ji Chen,[2] and Kezun Xu[2]
[1]*Department of Physics, Shanxi Normal University, Linfen, Shanxi 041004, People's Republic of China*
[2]*Department of Modern Physics, University of Science and Technology of China, Hefei, Anhui 230026, People's Republic of China*
(Received 3 July 1996; revised manuscript received 29 October 1996)

Triple differential cross sections (TDCS's) have been calculated for ionization of He^+ by electron impact in the coplanar asymmetric geometry for three different incident energies 250, 500, and 1000 eV, and fixed value of the ejected energy 5 eV and scattering angles (4° and 10°), and in the coplanar symmetric geometry for incident energies of 250–2000 eV as well. The final-state wave function used here considers all three two-body interactions and satisfies the proper asymptotic Coulomb boundary condition. The initial channel wave function involves a Coulomb wave due to the long-range Coulomb attraction between the incident electron and the screened ionic nucleus. Parts of the calculated TDCS's are compared with the existing theoretical results. [S1050-2947(97)08802-1]

PACS number(s): 34.80.Dp

I. INTRODUCTION

Electron-impact ionization of ions has attracted considerable attention in recent years from both experimental and theoretical physicists because of the increasing need for such data, particularly in the fields of astrophysics, controlled nuclear fusion, short wavelength laser development, and plasma physics. It is known that triple differential cross sections (TDCS's) give the most detailed information about the kinematics of such ionization processes. Unfortunately, no such experimental data have yet been obtained. The absence of any experimental data adds further importance to the theoretical study of such reaction. To our knowlege, the theoretical TDCS calculations for an electron-hydrogenic-ion ionization process were done by Roy, Roy, and Sil [1] and Biswas and Sinha [2]. The electron-electron correlation effect in the final channel was not considered in the calculations of Roy, Roy, and Sil. Consequently, the final-state wave function in their approach did not satisfy the proper asymptotic three-body boundary condition. In Ref. [2] Biswas and Sinha suggested a theoretical model for the calculation of the TDCS in which the faster outgoing (scattered) is treated in the framework of the eikonal approximation, while for slower electron (ejected) a Coulomb wave is considered. The correlation between the two outgoing electrons is taken into account via the eikonal phase term as well as through the Coulomb parameter occurring in the Coulomb wave. Therefore, final-state electronic interactions are presented in this model and, for the collision geometries considered in this work (high and intermediate incident energies with small momentum transfer), the work of Ref. [2] is a justfied approximation.

In the work of Brauner, Briggs, and Klar [3], hereafter referred to as BBK, a symmetric form of wave function was used to describe the three-body Coulomb continuum state resulting from electron-impact ionization of the hydrogen atom. A similar form of the correlated three-body wave function was first suggested by Garibotti and Miraglia [4] for proton-hydrogen impact, which consisted of a product of two plane waves describing the free internal motion of the three-body system, and was modified by a product of three Coulomb distortion factors describing the separate action of each of the three two-body potentials.

The BBK wave function is asymptotically correct when all interparticle separations are large, and the results are very good compared to experimental TDCS's of the hydrogen atom [5] at energies about ten times threshold or more. It is noted that in the BBK model all three particles in the final state are treated on an equal footing, the projectile-ejected-electron correlation is in detail considered and the proper three-body asymptotic boundary condition is satisfied.

In the present work, an extension of the BBK model to electron-impact ionization of ions is made. The TDCS's of ionization for hydrogenic ions are calculated in the intermediate- and high-energy regimes, with small momentum transfer for coplanar asymmetric and coplanar symmetric geometry. The incident electron is described by the Coulomb wave due to the long-range Coulomb attraction between the incident electron and the screened ionic nucleus, while the final channel is depicted by the BBK wave function. The final-state wave function considered here describes the large interparticle separations satisfactorily, and for such a situation also fulfills the correct Coulomb boundary condition. Although the present pattern is mainly based on the BBK model, a further complication arises in the theoretical calculation of the ionization of ions because of the long-range Coulomb interaction in the initial channel. As a test of this extension, we reinvestigate the scattering between the electron and the hydrogenic ion which was considered earlier in Ref. [2].

As far as we know, this is the first attempt to calculate the electron-ion collision cross section by the BBK model. In Sec. II the formula for the electron-imapct ionization is given. After a simple description of numerical procedures, a comparison with existing theoretical results is performed in Sec. IV. In this paper atomic units (a.u.) are used unless otherwise specified.

II. THEORY

The TDCS is given by

$$\frac{d^3\sigma}{d\Omega_1 d\Omega_2 dE_2} = (2\pi)^4 \frac{k_1 k_2}{k_i} |T_{fi}|^2, \tag{1}$$

where $\mathbf{k}_i$, $\mathbf{k}_1$, and $\mathbf{k}_2$ are the momenta of the incident, the scattered, and the ejected electrons, respectively. Ω_1 and Ω_2 are the detective solid angles of the two outgoing electrons with momenta $\mathbf{k}_1$ and $\mathbf{k}_2$, respectively. E_2 is the energy of the ejected electron. The T-matrix element is defined as

$$T_{fi}=\langle\Psi_f^-|V_i|\Psi_i^+\rangle, \tag{2}$$

where the projectile-target interaction V_i reads

$$V_i=\frac{1}{r_{12}}-\frac{1}{r_1} \tag{3}$$

where $r_{12}=\mathbf{r}_1-\mathbf{r}_2$, $\mathbf{r}_1$ and $\mathbf{r}_2$ are the projectile and the ejected electron position vectors, respectively, with respect to the target nucleus.

The initial channel wave function Ψ_i^+ which consists of the incident electron and the bound electron, will be described by the product of two wave function, one describing the incident electron and the other describing the bound electron. The incident electron will be given by the Coulomb wave $F_c(\mathbf{k}_i,\mathbf{r}_1)$ due to the long range Coulomb attraction between the incident particle and the screened target ion. Thus the initial state chosen as

$$\Psi_i^+=F_c(\mathbf{k}_i,\mathbf{r}_1)\phi_i(\mathbf{r}_2). \tag{4}$$

The Coulomb wave is given by

$$F_c(\mathbf{k}_i,\mathbf{r}_1)=(2\pi)^{-3/2}e^{\pi\alpha_i/2}\Gamma(1-i\alpha_i)e^{i\mathbf{k}_i\cdot\mathbf{r}_1}\times{}_1F_1(i\alpha_i;1;i(k_ir_1-\mathbf{k}_i\cdot\mathbf{r}_1)) \tag{5}$$

with $\alpha_i=(z-1)/k_i$, and $z(=2)$ is the charge of the target nucleus. The bound-state wave function of the ground state of He^+ is taken to be

$$\phi_i(\mathbf{r}_2)=\left(\frac{z^3}{\pi}\right)^{1/2}e^{-\lambda_ir_2}, \tag{6}$$

where λ_i $(=z)$ is the bound state parameter of the ground state of He^+.

The final-state wave function Ψ_f^- is the solution of the three-body problem which satisfies incoming-wave boundary condition and is considered here as given by the BBK [3],

$$\Psi_f^-=(2\pi)^{-3}e^{i\mathbf{k}_1\cdot\mathbf{r}_1}e^{i\mathbf{k}_2\cdot\mathbf{r}_2}C(\alpha_1,\mathbf{k}_1,\mathbf{r}_1)C(\alpha_2,\mathbf{k}_2,\mathbf{r}_2)\times C(\alpha_{12},\mathbf{k}_{12},\mathbf{r}_{12}), \tag{7}$$

where the Coulomb part of the wave function is defined as

$$C(\alpha,\mathbf{k},\mathbf{r})=e^{(1/2)\pi\alpha}\Gamma(1+i\alpha){}_1F_1(-i\alpha;1;-i(kr+\mathbf{k}\cdot\mathbf{r})) \tag{8}$$

and

$$\mathbf{k}_{12}=\tfrac{1}{2}(\mathbf{k}_1-\mathbf{k}_2),\quad \mathbf{r}_{12}=\mathbf{r}_1-\mathbf{r}_2,$$

$$\alpha_1=\frac{z}{k_1},\quad \alpha_2=\frac{z}{k_2},\quad \alpha_{12}=-\frac{1}{2k_{12}}. \tag{9}$$

To determine TDCS's we have to find T_{fi}, which is transformed as

$$T_{fi}=\lim_{\eta,\beta\to0^+}N\left[\frac{\partial^2}{\partial\lambda_i\partial\eta}-\frac{\partial^2}{\partial\lambda_i\partial\beta}\right]I, \tag{10}$$

where I is given by

$$I=\int\frac{d\mathbf{r}_1d\mathbf{r}_2}{r_1r_2r_{12}}e_1^{i\mathbf{q}\cdot\mathbf{r}_1-i\mathbf{k}_2\cdot\mathbf{r}_2-\eta r_1-\lambda_ir_2-\beta r_{12}}\times F_1(i\alpha_i;1;i(k_ir_1-\mathbf{k}_i\cdot\mathbf{r}_1))\times{}_1F_1(i\alpha_1;1;i(k_1r_1+\mathbf{k}_1\cdot\mathbf{r}_1))\times{}_1F_1(i\alpha_2;1;i(k_2r_2+\mathbf{k}_2\cdot\mathbf{r}_2))\times{}_1F_1(i\alpha_{12};1;i(k_{12}r_{12}+\mathbf{k}_{12}\cdot\mathbf{r}_{12})), \tag{11}$$

with $\mathbf{q}=\mathbf{k}_i-\mathbf{k}_1$ (momentum transfer), and

$$N=\frac{(2z^3)^{1/2}}{(2\pi)^5}\Gamma(1-i\alpha_i)\Gamma(1-i\alpha_1)\Gamma(1-i\alpha_2)\Gamma(1-i\alpha_{12})\times e^{(\pi/2)(\alpha_i+\alpha_1+\alpha_2+\alpha_{12})}. \tag{12}$$

Here we have introduced the parameters η and β for the convenience of our calculations.

Nordsieck [6] evaluated the integration of the product of two confluent hypergeometric function ${}_1F_1$ by the contour integration method in terms of the appropriate Gauss hypergeometric function ${}_2F_1$ with a real argument lying between 0 and 1. He evaluated the above integral in the matrix elements for the study of bremsstrahlung and pair production. The closed contour integral used by Nordsieck is taken to be

$${}_1F_1(i\alpha;1;z)=\frac{1}{2\pi i}\oint_\Gamma^{(0+,1+)}P(\alpha,t)e^{zt}dt \tag{13}$$

where $p(\alpha,t)=t^{-1+i\alpha}(t-1)^{-i\alpha}$, $p(\alpha,t)$ is single valued and analytic over the contour Γ enclosing 0 and 1 once anticlockwise, and there is a branch cut from 0 and 1. The phase convention is as follows: the phase of a complex variable z is to be taken as zero on the positive real axis, from which it is counted as positive when anticlockwise and negative when clockwise, there being a cut from 0 to $-\infty$ on the real axis. Applying this representation we may express Eq. (11) as

$$I=\left(\frac{1}{2\pi i}\right)^4\oint_{\Gamma_i}\oint_{\Gamma_1}\oint_{\Gamma_2}\oint_\Gamma dt_idt_1dt_2dtP(\alpha_i,t_i)P(\alpha_1,t_1)\times P(\alpha_2,t_2)P(\alpha_{12},t)J, \tag{14}$$

where

$$J=\int\frac{d\mathbf{r}_1d\mathbf{r}_2}{r_1r_2r_{12}}e^{-i\mathbf{p}_1\cdot\mathbf{r}_1}e^{i\mathbf{p}_2\cdot\mathbf{r}_2}e^{-\eta_1r_1}e^{-\eta_2r_2}e^{-\eta_{12}r_{12}}, \tag{15}$$

with

$$\eta_1=\eta-i(t_ik_i+t_1k_1),\quad \eta_2=\lambda-it_2k_2,\quad \eta_{12}=\beta-itk_{12}$$

$$\mathbf{p}_1=t_i\mathbf{k}_i-\mathbf{q}-t_1\mathbf{k}_1-t\mathbf{k}_{12},\quad \mathbf{p}_2=t_2\mathbf{k}_2-\mathbf{k}_2-t\mathbf{k}_{12}.$$

After performing the integration, J becomes

$$J=(4\pi)^2\int_0^\infty [As^2+2Bs+C]^{-1}ds, \tag{16}$$

where A, B and C are linear functions of t_1 and/or t_2, and have expressions similar to those given in Ref. [3], but the terms now involve t_i. Thus we can write $(As^2+2Bs+C)$ as $(\sigma_0+\sigma_1 t_1+\sigma_2 t_2+\sigma_{12}t_1t_2)$, where σ_0, σ_1, σ_2, or σ_{12} are functions of s, t_i, and t. Hence Eq. (16) can be recast into the following form:

$$J=(4\pi)^2\int_0^\infty [\sigma_0+\sigma_1 t_1+\sigma_2 t_2+\sigma_{12}t_1t_2]^{-1}ds. \tag{17}$$

From the two integral representations (14) and (17), we have

$$I=\frac{(4\pi)^2}{(2\pi i)^2}\int_0^{+\infty} ds \oint_{\Gamma_i} dt_i \oint_{\Gamma} dt P(\alpha_i,t_i)P(\alpha_{12},t)I_c(s,t_i,t), \tag{18}$$

where

$$I_c(s,t_i,t)=\frac{1}{(2\pi i)^2}\oint_{\Gamma_1}\oint_{\Gamma_2}\frac{dt_1dt_2P(\alpha_1,t_1)P(\alpha_2,t_2)}{\sigma_0+\sigma_1t_1+\sigma_2t_2+\sigma_{12}t_1t_2}. \tag{19}$$

I_c can be integrated by the residue theorem, which has been discussed in detail in Ref. [7], and finally we obtain

$$I_c(s,t_i,t)=\frac{1}{\sigma_0}\left(\frac{\sigma_0}{\sigma_0+\sigma_1}\right)^{i\alpha_1}\left(\frac{\sigma_0}{\sigma_0+\sigma_2}\right)^{i\alpha_2}{}_2F_1(i\alpha_1;i\alpha_2;1;Z), \tag{20}$$

where

$$Z=\frac{\sigma_1\sigma_2-\sigma_0\sigma_{12}}{(\sigma_0+\sigma_1)(\sigma_0+\sigma_2)}. \tag{21}$$

Although the form of I_c in Eq. (20) is similar to that given by Ref. [3] in Eq. (A30), it has involved some different parameters. The result which is obtained for $|Z|<1$ can be extended for any arbitrary value of Z by analytic continuation.

According to the analytic works of Mitra and Sil [8], the contour integrations in t_i and t occurring in Eq. (18) have been transformed into the following two-dimensional real integrals ranging from 0 to 1 or $-\infty$ to ∞, respectively:

$$N(s,t_i)=\frac{1}{2\pi i}\oint_\Gamma P(\alpha_{12},t)I_c(s,t_i,t)dt \tag{22}$$

$$=I_c(s,t_i,0)-\frac{\sinh(\pi\alpha_{12})}{i\pi}\int_0^1 dt\frac{I_c(s,t_i,t)-I_c(s,t_i,0)}{t}\times\left(\frac{1-t}{t}\right)^{-i\alpha_{12}} \tag{23}$$

$$=I_c(s,t_i,0)-\frac{\sinh(\pi\alpha_{12})}{i\pi}\int_{-\infty}^{\infty} dx\frac{e^{x-i\alpha_{12}x}}{1+e^x}\times\left[I_c\left(s,t_i,\frac{1}{1+e^x}\right)-I_c(s,t_i,0)\right] \tag{24}$$

and

$$U(s)=\frac{1}{2\pi i}\oint_{\Gamma_i}P(\alpha_i,t_i)N(s,t_i)dt_i \tag{25}$$

$$=N(s,0)+\frac{i\sinh(\pi\alpha_i)}{\pi}\int_0^1 dt_i\frac{N(s,t_i)-N(s,0)}{t_i}\times\left(\frac{1-t_i}{t_i}\right)^{-i\alpha_i} \tag{26}$$

$$=N(s,0)+\frac{i\sinh(\pi\alpha_i)}{\pi}\times\int_{-\infty}^{\infty}dy\frac{e^{y-i\alpha_i y}}{1+e^y}\left[N\left(s,\frac{1}{1+e^y}\right)-N(s,0)\right]. \tag{27}$$

Therefore, a three-dimensional integral is reached, and can be evaluated numerically to calculate T_{if}.

III. NUMERICAL INTEGRATION

For all the individual parts of integration the Gauss-Legendre quadrature method is applied. We first perform the s integration after an inverse transformation [i.e,. $v=1/(1+s)$]. The integral (ranging from 0 to 1) is evaluated by the Gauss quadrature method with different fixed values of t (or x) and t_i (or y) which are the coordinates of the Gauss-Legendre quadrature points required for the subsequent t (or x) and then t_i (or y) integrations. In these integrations the singularity at zero point are avoided by the method.

The Gauss hypergeometric function ${}_2F_1$ in Eq. (18) contains general complex argument. A technique to calculate the function over an entire complex plane has been developed by applying the linear transformations of the function [9] to ensure the efficiency and accuracy of evaluation.

In addition, the variables of η and β are introduced for convenience in the present calculations, and attention should be paid to the derivation of η and β. In the derivation of each variable, a forward-difference formula is utilized to keep the variable positive when it approaches zero. The covergence of each integral has been tested properly and the final results are supposed to be accurate up to data provided in the figures quoted in Sec. IV.

IV. RESULTS AND DISCUSSIONS

We have computed the TDCS's for electron impact ionization of $He^+(1s)$ for both symmetric and asymmetric geometries. In Figs. 1–3 we present the TDCS results for some selected set of dynamic parameters chosen in accordance with the existing theoretical work of Biswas and Sinha [2], i.e., at intermediate- and high-incident electron energies (250, 500, and 1000 eV) in coplanar and asymmetric geometry for fixed ejected energy 5 eV and fixed scattering angle 4° together with the corresponding ones of Biswas and Sinha against the angle θ_2 of the slower electron. For the highly asymmetric collisions the exchange effect between two continuum electrons is verified to be too small, so that it can be neglected safely.

As can be seen from the Figs. 1–3, the present TDCS results for He^+ (shown in full curves) are generally a bit smaller than the previous work [2] (dotted curves), but they

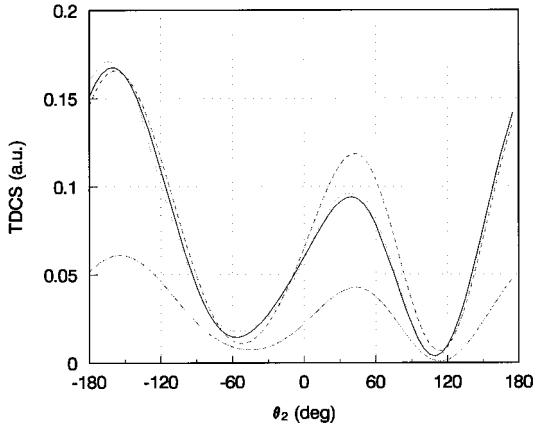

FIG. 1. The TDCS's (in a.u.) for the ionization of the He^+ ion form the ground state by electron impact, for the case when the incident energy $E_i=250$ eV, the ejected energy $E_2=5$ eV, and the scattering angle $\theta_1=4°$, as a function of ejected angle θ_2. The full curve shows the present TDCS results, the dotted curve shows the corresponding TDCS results of Biswas and Sinha [2], the broken curve the corresponding TDCS results for incident plane wave (i.e., for $\alpha_i=0$), and the chain curve the corresponding TDCS results for approximated BBK ($t=0$, $\alpha_i\neq 0$).

exhibit a similar angular distribution. The slight difference and similarity have also been encountered in the TDCS calculations of atomic hydrogen in Ref. [10]. Therefore, there are some inner connections between the eikonal approximate process for the scattered electron and the BBK model. Actually, the main difference between the two models is in the final-state wave function. It can be easily found from the models that the wave function used by Biswas and Sinha can be considered as an order approximate result of the BBK wave function, in the condition of the asymptotic region ($r_1, r_{12}\rightarrow\infty$ and short wavelength condition $k_1>>k_2$). Except for insignificant phase factors the BBK wave function reduces to Biswas and Sinha's. Therefore, in this geometry, the numerical results of the two models should not be distinguishable.

Figures 1–3 also contain the corresponding TDCS results

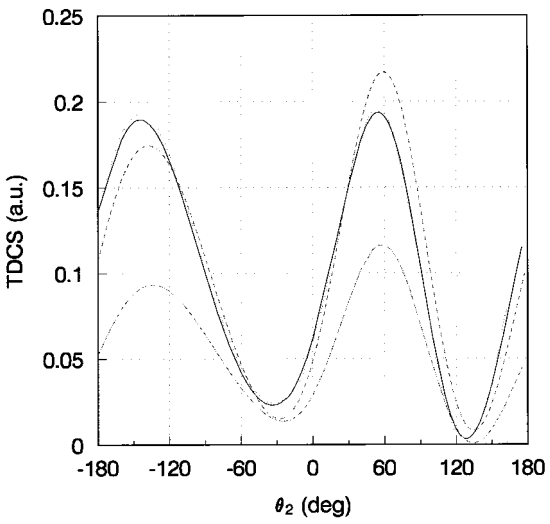

FIG. 2. Same as Fig. 1, but with $E_i=500$ eV.

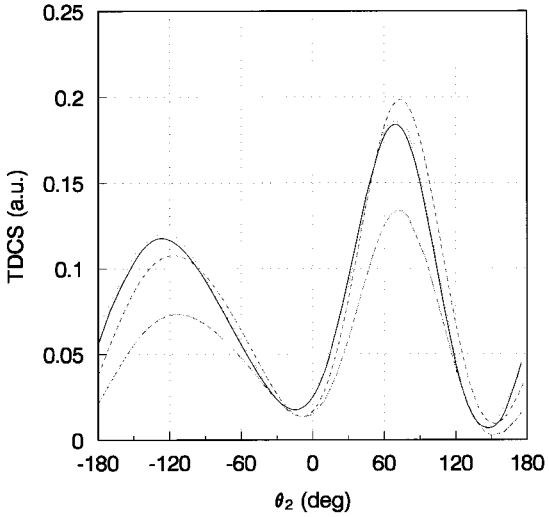

FIG. 3. Same as Fig. 1, but with $E_i=1000$ eV.

for which the incident Coulomb wave occuring due to the fact that the long-range interaction between the projectile and the ionic target is replaced by a plane wave (broken curves), and the BBK wave function is replaced by an approximate BBK model (chain curves) in which the third hypergeometric function in Eq. (11) is assumed to be equal to 1 and the repulsive factor $e^{(\pi/2)\alpha_{12}}\Gamma(1+i\alpha_{12})$ is kept. We have computed these results by individually setting parameters α_i and t in Eqs. (11)–(14) equal to zero in our general computer program.

The position of broken curves (plane-wave TDCS results) in Figs. 1–3 is always shifted with respect to the present results. The binary peaks are shifted toward larger angles, while the recoil peaks are shifted toward smaller angles. Since even at an energy as high as 1000 eV there is considerable difference between the present results and the TDCS results for an incident plane wave, it may be inferred that the long-range Coulomb interaction in the initial channel should not be neglected for ionization of an ionic target.

It may also be noted from Figs. 1–3 that TDCS's in the recoil and binary peaks are different between the incident plane-wave model and the present calculations. This discrepancy increases for decreasing impact energy. It demonstrates that the influence of the long-range Coulomb interaction in the initial channel is most prominent at lower incident energies. However, for the incident energies below 250 eV the BBK wave function describing the final state and the Coulomb wave used for the initial state should be modified by introducing the effective Sommerfeld parameters [11,12]. This work will be continued further.

An intense recoil peak is noted in the present TDCS curves for the He^+ ion as was found in the literature [2]. At a lower incident energy of 250 eV, the recoil peak is found to be even larger than the binary one (see Fig. 1). Since the recoil peak is mainly governed by the electron-nucleus interaction, the large recoil peak at the low energy of 250 eV may be qualitatively explained by strong elastic scattering from the nucleus (Avaldi, Camillon, and Stefani 1990 [13]). For higher incident energies of 500 and 1000 eV (see Figs. 2 and 3) the binary peak becomes stronger than the recoil peak.

In the approximate BBK results, the recoil and binary

peaks are always lower than the present results, however, a more or less similar angular distribution exists. The reason for this similarity is that in the approximate BBK model, we have kept the repulsive factor $e^{(\pi/2)\alpha_{12}}\Gamma(1+i\alpha_{12})$ which is sufficient to explain the strong angular correlation in the final state [14], although we have lost a part of information about the amplitude of the TDCS. Therefore, this approximate BBK model cannot only supply correct information about angular distributions, it also simplifies the compute pocedure for the study of electron-impact ionization of ions. In fact, Hda, Dal Cappello, and Langlois [14] made a similar extension to the case of $(e,3e)$ on atomic systems of Kr, Kr^{2+}, and Ar, which gives a good prediction for experiments.

While the TDCS for symmetric geometry cannot be yielded by the theoretical model of Biswas and Sinha [2], we also computed the TDCS for coplanar symmetric geometry with $\theta_1=\theta_2=45°$ at incident energies from 250 to 2000 eV (shown in the full curve of Fig. 4). Up to now, the only results for He^+ at incident energies of 200–2000 eV have been reported by Roy, Roy, and Sil (broken curve) [1]. In the present work we have repeated their results (in Fig. 4) through switching off the correlated part of the three-body Coulomb wave function.

In conclusion, we have performed a first Born calculation using correlated double-continuum wave functions for electron-impact ionization of positive ions. The results obtained show that the long-range Coulomb interaction in the initial channel should not be neglected for ionization of an ionic target. The present work can be applied for the TDCS estimate of ions at intermediate and high energies in asymmetric and symmetric geometry. This work opens the way to a determination of the TDCS for electron-impact ionization of positive ions, in which there is a great experimental interest.

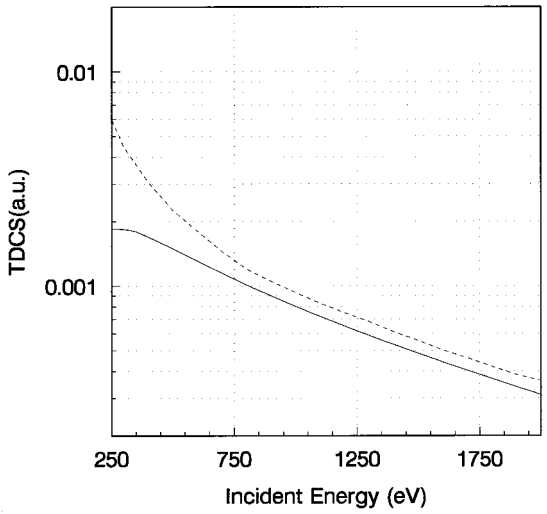

FIG. 4. The TDCS's (in a.u.) for the ionization of the He^+ ion by electron impact for coplanar symmetric geometry ($E_1=E_2$, $\theta_1=\theta_2=45°$) plotted against incident energy.

ACKNOWLEDGMENTS

This work was supported by the National Natural Science Foundation of China.

[1] A. Roy, K. Roy, and N. C. Sil, J. Phys. B **15**, 1289 (1982).
[2] R. Biswas and C. Sinha, Phys. Rev. A **50**, 354 (1994).
[3] M. Brauner, J. S. Briggs, and H. Klar, J. Phys. B **22**, 2265 (1989).
[4] G. Garibotti and J. E. Miraglia, Phys. Rev. A **21**, 572 (1980).
[5] H. Ehrhardt, K. Jung, G. Knoth, and P. Schlemmer, Z. Phys. D **1**, 3 (1986).
[6] A. Nordsieck, Phys. Rev. **93**, 785 (1954).
[7] K. Roy, P. Mandal, and N. C. Sil, Ind. J. Phys. B **68B**, R1 (1994).
[8] C. Mitra and N. C. Sil, J. Phys. B **25**, 1577 (1992).
[9] M. Abramowitz and I. A. Stegun, *Handbook of Mathematical Functions, Applied Mathematics Series*, 4th ed. (National Bureau of Standards, Washington, D.C., 1965), Vol. 55, p. 559.
[10] C. Sinha and S. Tripathi, J. Phys. B **24**, 3659 (1991).
[11] J. Berakar and J.S. Briggs, Phys. Rev. Lett. **72**, 3799 (1994).
[12] J. Berakar, Phys. Rev. A **53**, 2314 (1996).
[13] L. Avaldi, R. Camilloni, and G. Stefani, Phys. Rev. A **41**, 134 (1990).
[14] H. Hda, C. Dal Cappello, and J. Langlois, Z. Phys. D **29**, 25 (1994).